https://doi.org/10.5194/esurf-2020-67
Preprint. Discussion started: 8 September 2020

Earth Surface Dynamics Discussions

Effect of stress history on sediment transport and channel adjustment in graded gravel-bed rivers

Chenge An[1,2], Marwan A. Hassan[2], Carles Ferrer-Boix[3], Xudong Fu[1]

[1] Department of Hydraulic Engineering, State Key Laboratory of Hydroscience and Engineering, Tsinghua University, Beijing, China.
[2] Department of Geography, The University of British Columbia, Vancouver, BC, Canada.
[3] Department of Civil and Environmental Engineering, Technical University of Catalonia, Barcelona, Spain.

Correspondence to: Xudong Fu (xdfu@tsinghua.edu.cn)

Abstract. With the increasing attention on environmental flow management for the maintenance of habitat diversity and ecosystem health of mountain gravel-bed rivers, much interest has been paid to how inter-flood low flow can affect gravel-bed river morphodynamics during subsequent flood events. Previous research has found that antecedent conditioning flow can lead to an increase in the critical shear stress and a reduction in sediment transport rate during a subsequent flood. But how long this effect can last during the flood event has not been fully discussed. In this paper, a series of flume experiments with various durations of conditioning flow are presented to study this problem. Results show that channel morphology adjusts significantly within the first 15 minutes of the conditioning flow, but becomes rather stable during the remainder of the conditioning flow. The implementation of conditioning flow can indeed lead to a reduction of sediment transport rate during the subsequent hydrograph, but such effect is limited only within a relatively short time at the beginning of the hydrograph. This indicates that bed reorganization during the conditioning phase, which induce the stress history effect, is likely to be erased with increasing intensity of flow and sediment transport during the subsequent flood event.

1 Introduction

Prediction of sediment transport is of vital importance because it is related to many aspects of river dynamics and management, including river morphodynamics modeling (Parker, 2004), river restoration (Chin et al., 2009), aquatic habitats (Montgomery et al., 1996), natural hazard planning (Marston, 2008), bedrock erosion (Sklar and Dietrich, 2004), and landscape evolution (Howard, 1994). In mountain gravel-bed rivers, sediment transport is controlled by flow magnitude and flashiness, sediment supply, bed surface structures, channel morphology and the grain size distribution (GSD) of sediment (Montgomery and Buffington, 1997). Therefore, prediction of sediment transport in mountain rivers still remains difficult despite the large body of existing theories. This is due to the fact that these theories were mostly developed for lowland streams with continuous sediment supply and an average flow regime, which do not apply to mountain streams (Gomez and Church, 1989; Rickenmann, 2001; Schneider et al., 2015).

For example, the hydrograph of mountain gravel-bed rivers is often characterized by large fluctuations of flow discharge, including both short-term flash flood and long-term inter-flood low flow (Powell et al., 1999). However, research on the morphodynamics of mountain rivers often focuses on the effects of floods (or constant high flow) and neglects the role of inter-flood low flow, with the consideration that most sediment transport and morphological adjustments of mountain rivers occur during relatively high flows (Klingeman and Emmett, 1982; Paola et al., 1992).

Reid and colleagues (Reid and Frostick, 1984; Reid et al., 1985) studied the effects of inter-flood low flow on subsequent sediment transport in Turkey Brook, England. They found that bedload transport rates were reduced during relatively isolated flood events (e.g., events separated by long time intervals) compared to those that were closely spaced, with the entrainment threshold up to as large as three times higher. They linked this with sediment reorganization during prolonged periods of antecedent flow, which can make the river bed more armored and more resistant to entrainment, thus delaying the onset of sediment mobility in the following flood event.

To further study such "memory" effect of antecedent flow on the sediment transport during a subsequent flood, a number of flume experiments as well as field surveys have been conducted in the past decade, and different terms have been proposed, including "stress history effect" (Monteith and Pender, 2005; Paphitis and Collins, 2005; Haynes and Pender, 2007; Ockelford and Haynes, 2013), "flood history effect" (Mao, 2018), "flow history" (Masteller et al., 2019), etc. Given that all these terms are similar, here we adopt the term "stress history" in this paper.

Paphitis and Collins (2005) conducted flume experiments to study the entrainment threshold of uniform sediment subjected to antecedent flow durations of up to 120 minutes. They found that with a longer and higher antecedent flow, the critical bed shear stress increases and the total bedload flux decreases. The work of Paphitis and Collins (2005) was extended by Monteith and Pender (2005) and Haynes and Pender (2007) to consider bimodal sand-gravel mixtures. They found that for a graded bed, longer periods of antecedent flow increase bed stability due to local particle rearrangement, in agreement with Paphitis and Collins (2005); whereas higher magnitudes of antecedent flow reduce bed stability due to selective entrainment of the fine matrix on bed surface, counter to Paphitis and Collins' (2005) conclusion based on uniform sediment. Hayes and Pender (2007) further analyzed the two competing effects and concluded that particle rearrangement may be of greater relative importance than the winnowing of the fine sediment as it affects subsequent sediment transport. By using high resolution laser scanning and statistical analysis of the bed topography, Ockelford and Haynes (2013) also demonstrated that the response of bed topography to stress history is grade specific: bed roughness decreased in uniform beds but increased in graded bed with an increase length of an antecedent flow period. Performing a series of flume experiments, Masteller and Finnegan (2017) studied the evolution of the river bed on particle scale during low flow. They linked reduction of bedload flux to the re-organization of the highest protruding grains (1%-5% of the entire bed) on bed surface.

Because of the above-mentioned research, existing sediment transport formulae for gravel-bed rivers (e.g. Meyer-Peter and Müller, 1948; Parker, 1990; Wilcock and Crowe, 2003; Wong and Parker, 2006) are regarded to be inaccurate because they do not take the effect of stress history into account. To this end, Paphitis and Collins (2005) proposed an empirical formula for the exposure correction factor in the critical shear velocity for a uniform sand-size bed based on their experimental

https://doi.org/10.5194/esurf-2020-67
Preprint. Discussion started: 8 September 2020

Earth Surface Dynamics Discussions

data. Johnson (2016) developed a state function for the critical shear stress in terms of transport disequilibrium, which incorporates the effects of stress history and hydrograph variability. Ockelford et al. (2019) proposed two forms of functions to link the antecedent duration and the critical shear stress. The two alternatives proposed by Ockelford et al. (2019) correct the function proposed by Paphitis and Collins (2005), whose exposure correction uses a logarithmic function which implicitly assumes an unbound growth as antecedent time tends towards infinity.

Research to date has shown that antecedent flow can stabilize the river bed, thus influencing the threshold of sediment motion as well as bedload flux. However, most of the previous research about stress history is either under conditions with relatively low sediment transport or with relatively short durations of sediment transport in order to capture the threshold of sediment motion (Monteith and Pender, 2005; Paphitis and Collins, 2005; Haynes and Pender, 2007; Ockelford and Haynes, 2013; Masteller and Finnegan, 2017; Ockelford et al., 2019). On the other hand, other researchers have found that exceptionally high discharge events can reduce critical shear stress by disrupting particle interlocking and breaking of bed structure (Turowski et al., 2011; Yager et al., 2012; Ferrer-Boix and Hassan 2015; Masteller et al., 2019). Flume experiments by Masteller and Finnegan (2017) also indicate an increase in the number of highly mobile, highly protruding grains in response to sediment transporting flows. Therefore, the effect of high discharge events in reducing the critical shear stress likely counterbalances the stress history effect of antecedent flow to increase the critical shear stress. In consideration of these opposing mechanisms, how long can the stress history effect last during a subsequent flood event is not well understood. Such a question is important especially in light of the fact that most sediment transport and channel adjustment of mountain gravel-bed rivers occurs during high discharge events, when the flow shear stress is high.

In this paper, flume experiments consisting of extended cycles of high and low flow is conducted to study this problem. The experimental arrangement is described in Sect. 2. In Sect. 3, we present the experimental results showing how channel morphology and sediment transport during a subsequent hydrograph respond to various durations of antecedent conditioning flow. The threshold of motion is analyzed in Sect. 4 based on the experimental data. Implications and limitations of this study are also discussed in Sect. 4. Finally, conclusions are summarized in Sect. 5.

2 Experimental arrangements

The experimental arrangements were guided by conditions observed in East Creek, a small mountain creek in Malcom Knob Forest, University of British Columbia (for details on the study site see Papangelakis and Hassan, 2016). To investigate study objectives, we conducted flume experiments in the Mountain Channel Hydraulic Experimental Laboratory at the University of British Columbia. The experiments were conducted in a tilting flume with a length of 5 m, a width of 0.55 m and a depth of 0.80 m. The initial slope was 0.04 m/m. Water, but not sediment was recirculated by an axial pump. A set of six experiments (REF2 – REF7) was conducted; the experimental conditions are briefly summarized in Table 1. For experiments REF3 – REF7, the same hydrograph and sedimentograph were conducted, but with different durations of constant conditioning flow prior to the hydrograph/sedimentograph. We denote these as REF3 (10), REF4 (2), REF5 (5), REF6 (15)

https://doi.org/10.5194/esurf-2020-67
Preprint. Discussion started: 8 September 2020

and REF7 (0.25), with the numbers in the brackets denoting the duration of the conditioning flow in hours. Experiment REF2 (15) consists of a 15-hour conditioning period without a subsequent hydrograph/sedimentograph, to test the reproducibility of our experimental results during the conditioning flow.

https://doi.org/10.5194/esurf-2020-67
Preprint. Discussion started: 8 September 2020

Table 1. Summary of the experimental conditions and measurements. The experiments are listed in the table in order of decreasing duration of conditioning flow.

No.	Phase	Duration (h)	Flow discharge (l/s)	Water surface slope (%)	Flow depth (cm)	Froude number (-)	τ_b (Pa)	Sediment feed (kg/h)	D_{s50} (mm)	D_{s90} (mm)	D_{l50} (mm)	D_{l90} (mm)	τ^*_{s50}	Q_s (kg/h)
REF2 (15)	Conditioning	15	25	2.62	6.33	0.91	16.27	0	15.2	29.6	1.07	5.43	0.069	0.27
REF6 (15)	Conditioning	15	25	3.27	6.47	0.88	20.76	0	15.87	30.69	35.18	42.84	0.089	0.89
	Step 1	2	26	3.34	6.39	0.94	20.93	1	15.66	29.98	12.51	39.38	0.083	0.68
	Step 2	2	28	3.10	6.29	1.03	19.13	1.5	17.18	30.40	7.28	27.59	0.069	0.76
	Step 3	2	32	3.06	6.80	1.05	20.41	3.2	15.34	30.85	12.39	36.54	0.082	6.73
	Step 4	2	40	2.81	7.78	1.07	21.45	10	15.95	30.34	11.48	36.03	0.083	13.39
REF3 (10)	Conditioning	10	25	2.73	6.02	0.98	16.12	0	14.9	29.5	2.17	9.98	0.071	0.28
	Step 1	2	26	2.75	5.93	1.04	16.00	1	15.0	29.3	2.55	19.94	0.066	1.71
	Step 2	2	28	2.69	6.35	1.01	16.77	1.5	15.5	29.7	4.06	26.99	0.067	2.19
	Step 3	2	32	2.88	6.81	1.04	19.25	3.2	15.9	29.7	6.18	24.26	0.075	2.44
	Step 4	2	40	2.48	8.34	0.96	20.28	10	15.6	32.8	14.45	39.13	0.080	12.45
REF5 (5)	Conditioning	5	25	3.26	5.51	1.12	17.63	0	16.35	31.14	8.23	25.34	0.066	0.49
	Step 1	2	26	3.24	6.19	0.98	19.68	1	16.30	30.90	6.57	23.63	0.075	2.24
	Step 2	2	28	3.09	6.21	1.05	18.82	1.5	16.87	31.27	9.38	28.44	0.069	3.30
	Step 3	2	32	3.05	6.65	1.08	19.91	3.2	16.04	31.04	11.90	47.91	0.077	5.72
	Step 4	2	40	2.78	7.82	1.06	21.33	10	14.72	31.44	15.09	38.56	0.090	40.03
REF4 (2)	Conditioning	2	25	2.82	5.55	1.11	15.34	0	13.58	28.78	3.10	15.79	0.070	1.50
	Step 1	2	26	2.73	5.55	1.16	14.85	1	14.61	28.83	3.90	20.31	0.063	0.96
	Step 2	2	28	2.71	6.19	1.06	16.46	1.5	15.44	29.09	6.28	46.76	0.066	2.41
	Step 3	2	32	3.15	6.85	1.04	21.15	3.2	14.44	28.65	17.34	37.76	0.091	26.73
	Step 4	2	40	2.76	8.01	1.02	21.69	10	14.06	30.22	10.88	35.45	0.095	5.23
REF7 (0.25)	Conditioning	0.25	25	3.46	6.20	0.94	21.06	0	14.67	30.10	10.54	28.03	0.089	19.44
	Step 1	2	26	3.20	6.54	0.90	20.53	1	15.52	30.86	7.11	28.91	0.082	3.48
	Step 2	2	28	3.14	6.58	0.96	20.27	1.5	16.62	31.33	6.91	30.73	0.075	2.52
	Step 3	2	32	3.12	7.00	1.00	21.41	3.2	14.89	30.78	10.09	37.40	0.089	12.32
	Step 4	2	40	2.73	8.29	0.97	22.19	10	17.68	36.20	12.13	30.78	0.078	16.80

https://doi.org/10.5194/esurf-2020-67
Preprint. Discussion started: 8 September 2020

a. Q_s: bedload transport rate, τ_b: shear stress, D_{s50} and D_{s90}: D_{50} and D_{90} of bed surface, D_{l50} and D_{l90}: D_{50} and D_{90} of bedload, τ^*_{s50}: Shields number for D_{s50}. Here D_{90} denotes the grain size such that 90% is finer, and D_{50} denotes the grain size such that 50% is finer.

https://doi.org/10.5194/esurf-2020-67
Preprint. Discussion started: 8 September 2020

Figure 1 shows the water and sediment supply implemented in the experiments. The water discharge was selected to represent typical flows in East Creek, with the 25 l/s flow during the conditioning period being equivalent to half the bankfull flow, and the peak flow discharge of 40 l/s during the hydrograph being about 1.1 times the bankfull flow in East Creek. Because the purpose of this paper is to study the evolution of bed stability, sediment was not feed during the conditioning flow. For each step of the hydrograph, we chose a feed rate through numerical simulations following Ferrer-Boix and Hassan (2014) in combination with trial experiments. Sediment was fed into the flume at the upstream end using a conveyor belt feeder at the calculated transport rate capacity. The feed rate of the sedimentograph ranged between 1 kg/hour and 10 kg/hour. Both the hydrograph and the sedimentograph consisted of four steps, with each step lasting for 2 hours.

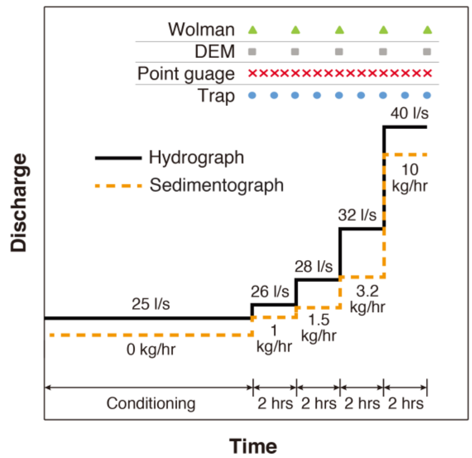

Figure 1. Water and sediment supply implemented in the experiments. Markers in top of the figure denote the time of measurements during the hydrograph phase. Time of measurements during the conditioning phase is not shown in this figure.

Figure 2 shows the GSD of the bulk sediment used in the experiments, with the grain size ranging between 0.5 and 64 mm. The GSD was scaled from East Creek by a ratio of 1:4, except that sediment (after scaling) with a grain size less than 0.5 mm was excluded. This preserved the entire gravel distribution of East Creek with a maximum size of 256 mm (scaled to 64 mm in Fig. 2). The model was "generic" rather than specific in that no attempt was made to reproduce the geometric details of the prototype channel. The bulk sediment was sieved in half φ intervals and painted in different colors for each size class for texture analysis and visual identification. Before the commencement of each experiment, we hand-mixed and screeded the bulk sediment to make a flat layer of loose material with a depth of 0.15 m. The sediment was then slowly flooded and then drained to aid settlement. The bulk sediment is also used for the sediment feed in each experiment.

https://doi.org/10.5194/esurf-2020-67
Preprint. Discussion started: 8 September 2020

Earth Surface Dynamics
Discussions
Open Access

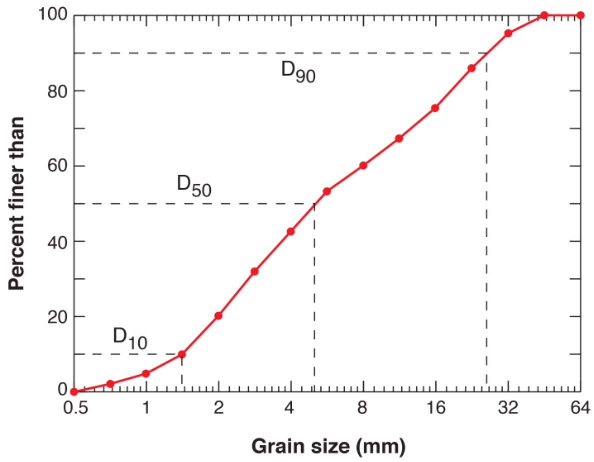

Figure 2. Grain size distribution of the bulk sediment used in the experiments.

The elevations of the bed surface and water surface were measured along the flume every 0.25 m using a mechanical point gauge with a precision of ±0.001 m. Water depth fluctuations due to wave effects at a point were about 5% or less. Water surface slope and bed slope are calculated based on a regression of the point gauge data measured between 0.5 m and 4.75 m upstream of the outlet. The most upstream and downstream sections are excluded to avoid boundary effects. A green laser scanner mounted on a motorized cart was also used to measure the bed surface elevation along the flume. Bed laser scans were composed of cross sections spaced 2 mm apart with 1 mm vertical and horizontal accuracy (for details see Elgueta-Astaburuaga and Hassan, 2017). The standard deviation of bed elevation was calculated based on the DEM data from scans. Before the calculation of standard deviation, the DEM was detrended to remove spatial trends with scales larger than the scale of sediment patterns (e.g., bed slope or undulations). To estimate the particle size distribution of the bed surface we used digital cameras mounted on a motorized cart along the entire flume. Images were merged together to visualize the bed and preform the particle size analysis (Chartrand et al., 2018). The particle size distribution of the bed surface was estimated using the grid by number (point counts) method, by identifying particle size at the intersection of a 5 cm grid superimposed on each photograph. Individual grains were identified by color. Collected data were used to quantify changes in the bed surface particle size distribution throughout each experiment.

Material evacuated from the flume was trapped in a 0.25 mm mesh screen in the tailbox, and weighted and sieved at half φ intervals to calibrate a light table. The sediment transport rates for various size ranges were measured at the end of the flume using a light table and automated image analysis at a resolution of 1 second (for details see Zimmerman et al., 2008; Elgueta-Astaburuaga and Hassan 2017). To avoid random fluctuations in sediment transport, we report the bedload transport rate at a 5-minute resolution, and characteristic grain sizes of bedload at 15-minute resolution. A range of methods for the estimation of bed shear stress has been suggested in the literature (reviewed in Whiting and Dietrich, 1990). In this study, the shear stress is estimated using the depth-slope product corresponding to normal (steady and uniform) flow. This method is selected because the focus of this work is on overall (mean) parameters controlling bed evolution; in addition, the water was too shallow to use an ADV. The water surface slope,

https://doi.org/10.5194/esurf-2020-67
Preprint. Discussion started: 8 September 2020

Earth Surface Dynamics Discussions

rather than bed slope, is implemented in the calculation of shear stress, with the consideration that water surface slope is closer to the friction slope and also has less random fluctuations than bed slope.

The frequency of measurements during the hydrograph phase is also plotted in Fig. 1(a), with the point gauge measurements conducted every 30 minutes, the trap weighting/sampling conducted every hour, and the DEM/Wolman measurements by laser scan/photograph conducted every 2 hours (i.e. at the beginning/end of each stage of the hydrograph). For each measurement of DEM/Wolman, the flow was slowly lowered and then stopped to allow for the bed to be scanned by a laser and photographed. The frequency of measurement during the conditioning phase was adjusted in each experiment in accordance with the duration of the conditioning phase, and is therefore not plotted in Fig. 1(a).

3 Experimental results

Table 1 presents an overall schematization of the experimental results, including water surface slope, flow depth h, Froude number F_r ($F_r = u / (gh)^{0.5}$), where u is depth-averaged flow velocity), bedload transport rate Q_s, shear stress τ_b, D_{50} and D_{90} of bed surface (D_{s50} and D_{s90}), D_{50} and D_{90} of bedload (D_{l50} and D_{l90}), and Shields number τ^*_{s50} for a given D_{s50}. Here D_{90} denotes the grain size such that 90% is finer, and D_{50} denotes the grain size such that 50% is finer.

3.1 Channel adjustment

In this section, we present the channel adjustments during each experiment. Figure 3 shows the difference of longitudinal DEM averaged over the cross section, which can represent the adjustment of channel topography during different periods of the experiment. From Fig. 3(a) we can see that for each experiment, evident degradation occurs during the first 15 minutes, especially at the upstream of the flume. This is due to the fact that no sediment supply is implemented during the conditioning period, and also the initial bed material is relatively loose. From 15 minutes until the end of the conditioning phase (as shown in Fig. 3(b)), no evident aggradation/degradation is observed for any experiment, indicating that most of the adjustment of channel topography during the conditioning phase has been accomplished within the first 15 minutes. For Step 1 of the hydrograph (as shown in Fig. 3(c)), no evident aggradation/degradation is observed for any of the experiments, except for REF7 (0.25), which has the shortest conditioning phase. Similarly, the channel keeps relatively stable during Step 2 of the hydrograph for all experiments (as shown in Fig. 3(d)), with no trend for aggradation/degradation observed. With the increase of flow discharge, some degradation (with a magnitude of about 10 ~ 20 mm) can be observed in Step 3 for all experiments at the upstream end of the channel, as shown in Fig. 3(e). Such degradation becomes more evident over the entire channel in Step 4 of the hydrograph, when flow discharge reaches its peak value. Further analysis of the DEM data shows that no bedform were evident during the experiment.

https://doi.org/10.5194/esurf-2020-67
Preprint. Discussion started: 8 September 2020

Earth Surface Dynamics
Discussions
Open Access

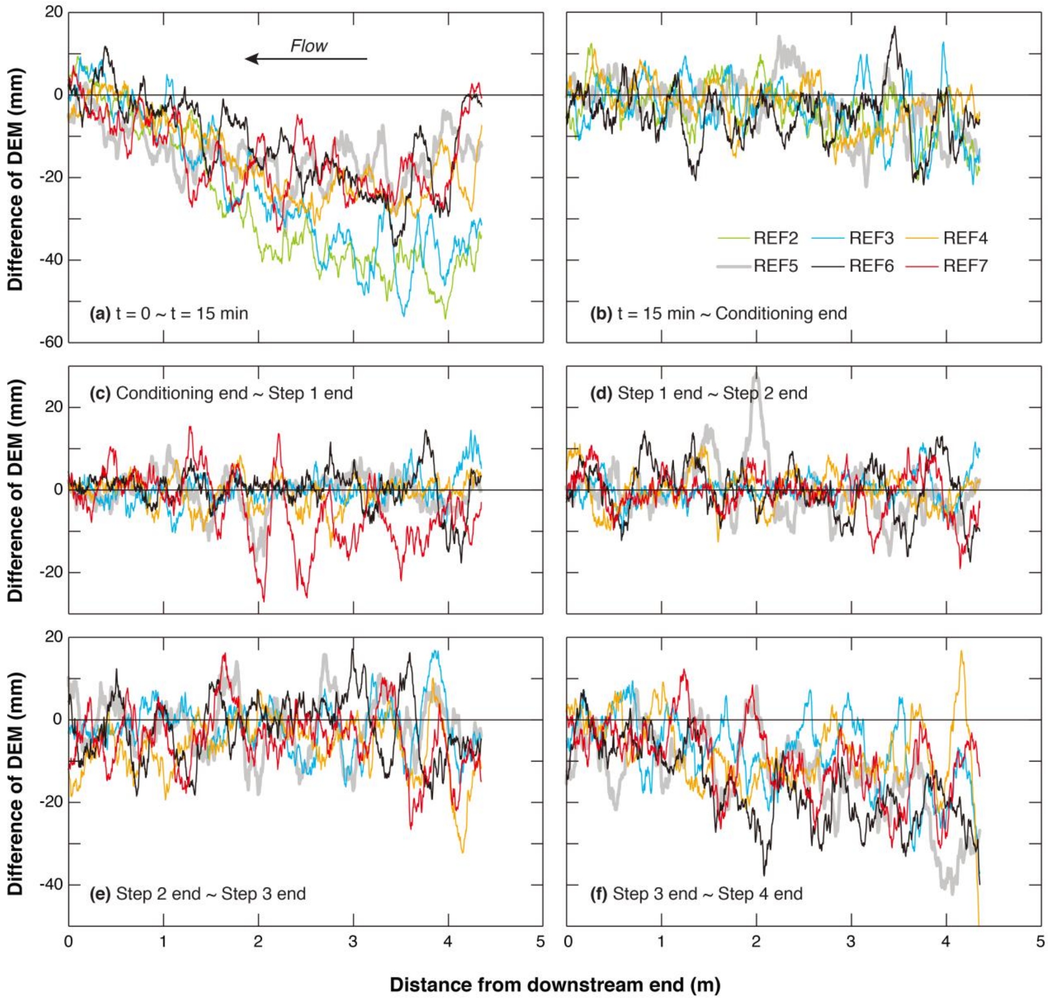

Figure 3. Spatial distribution of elevation difference from cross-sectionally averaged longitudinal DEM during the experiment: (a) from beginning of experiment to t = 15 minutes; (b) from t = 15 minutes to the end of conditioning phase; (c) from the end of conditioning phase to the end of Step 1 of hydrograph phase; (d) from the end of Step 1 to the end of Step 2 of the hydrograph phase; (e) from the end of Step 2 to the end of Step 3 of the hydrograph phase; (f) from the end of Step 3 to the end of Step 4 of the hydrograph phase.

Figure 4 shows the temporal variation of the standard deviation of bed elevation over the length of erodible bed during the experiment. Results show that the standard deviation of bed elevation is relatively small at the beginning of the experiments (corresponding to a relatively smooth bed depending on the way we prepared the initial bed), but increases notably within 15 minutes after the start of the conditioning phase. Such an increase of the bed roughness is accompanied by significant degradation during the first 15 minutes, as shown in Fig. 3(a). The standard deviation of bed elevation remains almost constant during the remaining conditioning phase, as well as during the hydrograph

https://doi.org/10.5194/esurf-2020-67
Preprint. Discussion started: 8 September 2020

phase, despite the fact that degradation is evident as the flow approaches its peak value. Besides, the value of standard deviation is almost identical for each experiment, indicating the period of conditioning phase exerts little effect on the standard deviation of bed elevation.

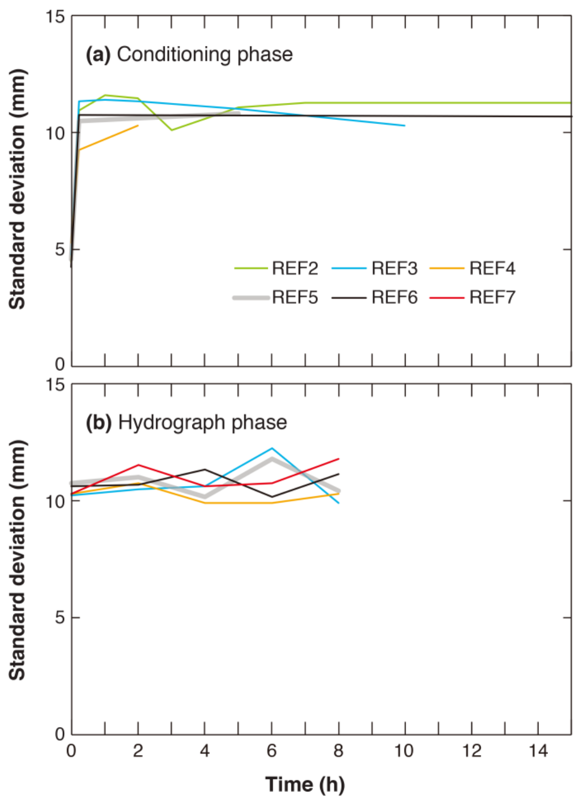

Figure 4. Temporal adjustments of standard deviation of bed elevation calculated over the whole erodible bed: (a) the conditioning phase; (b) the hydrograph phase.

Figure 5 shows the temporal variation of the characteristic grain size of bed surface material. Three parameters are presented here; D_{s10}, D_{s50}, and D_{s90}. The adjustment of bed surface GSD follows similar trends as the adjustment of standard deviation of bed elevation. For all experiments, the bed surface is fine at the beginning, and experiences a fast coarsening period during the first 15 minutes (along with the bed degradation in Fig. 3 and the increase of bed roughness in Fig. 4). The characteristic grain sizes of bed surface remain relatively stable after the first 15 minutes. It is worth noted that the GSD of bed surface keeps relatively constant even during the hydrograph phase, during which a flood event is introduced in the flume and evident bed degradation is observed. This is in agreement with the observation of Ferrer-Boix and Hassan (2015) during successive water pulses.

https://doi.org/10.5194/esurf-2020-67
Preprint. Discussion started: 8 September 2020

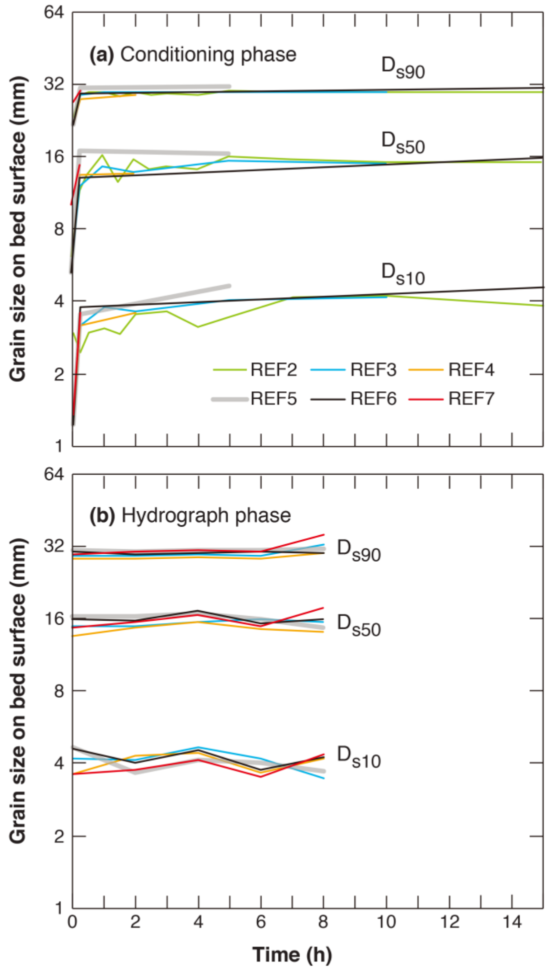

Figure 5. Temporal adjustments of characteristic grain sizes of bed surface material calculated over the whole erodible bed: (a) the conditioning phase; (b) the hydrograph phase.

3.2 Sediment transport

In Fig. 6 we exhibit the instantaneous sediment transport rate Q_s measured by the light table in each experiment. Sediment transport is reported every 5 minutes, as described in Sect. 2. It can be seen in Fig. 6(a) that the temporal variation of sediment transport rate during the conditioning phase follows the same trend in all six experiments. That is, the sediment transport rate decreases significantly during the conditioning phase, with the decreasing rate being very large at the beginning and then gradually dropping. The sediment transport rate eventually approaches a small and relatively constant value after about 8 hours of conditioning flow. Nevertheless, there are random high points in the sediment transport rate even after 8 hours, despite no sediment feed from the inlet. These spikes imply that partial destruction (or reorganization) of the bed structure occurs even after a long duration of conditioning.

https://doi.org/10.5194/esurf-2020-67
Preprint. Discussion started: 8 September 2020

Earth Surface Dynamics Discussions

Previous researchers (Haynes and Pender, 2007; Masteller and Finnegan, 2017) have suggested that an exponential function can be implemented to describe such a decrease of sediment transport rate under conditioning flow. Additional analysis is implemented in the Supporting Information to fit REF2 (15) and REF6 (15) (which have the longest duration of conditioning phase) against a two-parameter exponential function. Results show that the exponential function can describe the general decreasing trend of sediment transport rate during the conditioning phase, except at the beginning of the experiment where the decrease of sediment transport rate is much more significant than that predicted by the exponential function. Readers can refer to the Supporting Information for more details.

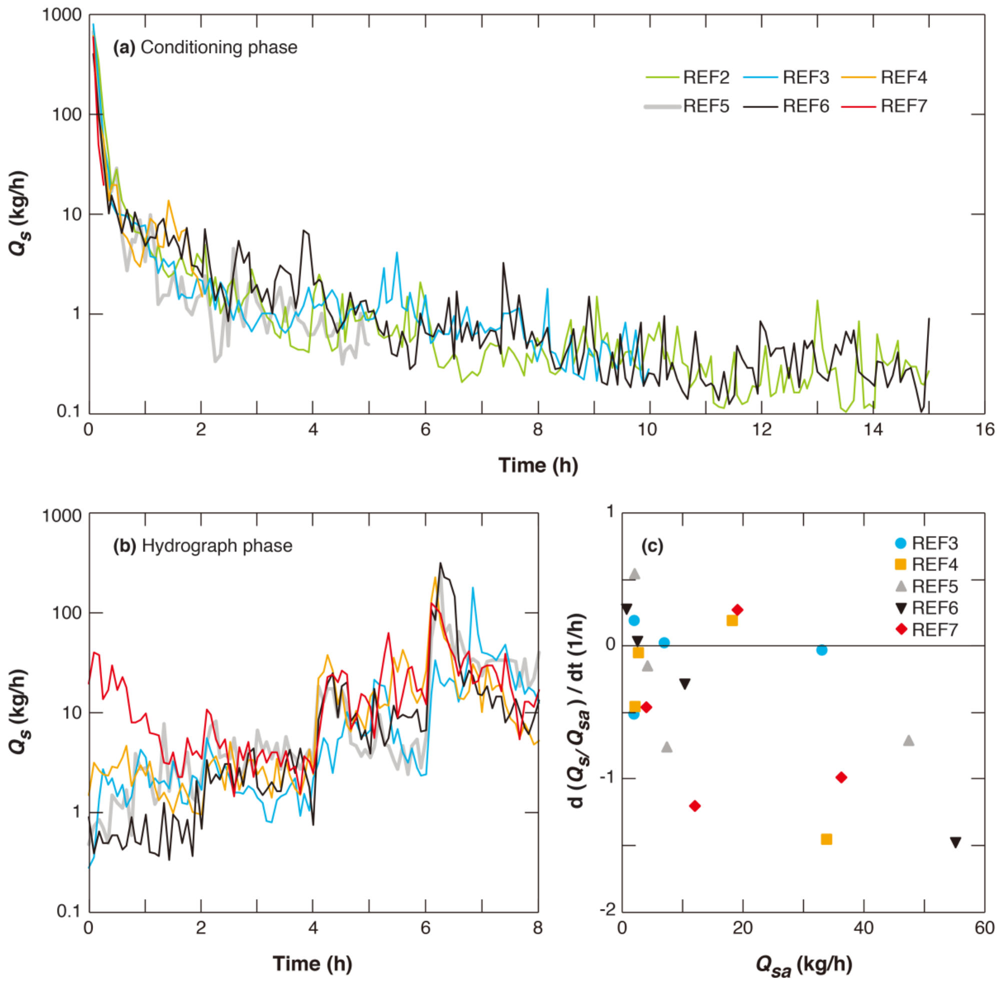

Figure 6. Instantaneous sediment transport rate measured by light table during (a) the conditioning phase; and (b) the hydrograph phase. (c) Intra-step temporal change rate of Q_s normalized against Q_{sa} for each hydrograph step. Q_s is the sediment transport rate, and Q_{sa} is the averaged sediment transport rate of a given hydrograph step.

https://doi.org/10.5194/esurf-2020-67
Preprint. Discussion started: 8 September 2020

Figure 6(b) presents the instantaneous sediment transport rate during the hydrograph phase. Results show that variation of sediment transport rate among different experiments prevails in the first step of the hydrograph, with the highest sediment transport rate for the experiment with the shortest conditioning duration (REF7 (0.25)); and the smallest sediment transport rate for the experiment with the longest conditioning duration (REF6 (15)). Such variation among experiments, however, diminishes towards the end of Step 1 and is not observed in the following three steps of the hydrograph, with the line for each experiment collapsing together in the figure. The adjustments of sediment transport rate agree with the channel deformation shown in Fig. 3, where the pattern of variation in REF7 (0.25) deviates from other experiments in Step 1 (more degradation in REF7 (0.25)), but collapses with other experiments in the following three steps.

Results in Fig. 6(b) also show large variations of sediment transport rate during each step of the hydrograph. Such intra-step variations of sediment transport rate are investigated in Fig. 6(c), with the x axis being the averaged sediment transport rate of each step Q_{sa} and the y axis being $d(Q_s/Q_{sa})/dt$, which is estimated by linear regression. Here the instantaneous sediment transport rate Q_s is scaled against the average sediment transport rate of the corresponding step Q_{sa}, in order to facilitate the comparison among different hydrograph steps.

Results in Fig. 6(c) shows that a large fraction of the data (11 out of 20) exhibits a decreasing trend in time for Q_s (i.e. a negative value in vertical coordinate). Basically, the larger the averaged sediment transport rate Q_{sa}, the larger is the rate of reduction in Q_s. Ferrer-Boix and Hassan (2015) observed similar declines in sediment transport during their water pulses experiments. They attributed this to (1) the presence of bed structures, which could have reduced skin friction up to 20% and (2) streamwise changes in the patterns of bed surface sorting. Out of 20 datasets, 5 exhibit some temporally increasing trend in Q_s (though not as evident as the decreasing trend mentioned before). They are REF5 (5), REF3 (10), REF6 (15) during the first step; and REF7 (0.25), REF4 (2) during the third step. This shows that for the three experiments with long conditioning duration, Q_s is very low at the end of the conditioning phase, and the first step of the hydrograph sees a temporally increasing trend in Q_s. Whereas for the two experiment with short conditioning phase, Q_s is still high at the end of the conditioning, so that the sediment transport rate keeps decreasing during the first step, until in the third step an increasing trend in Q_s is observed, at which the water and sediment supply become evidently higher.

To better understand the effect of the conditioning duration on sediment transport, we calculate the cumulative sediment transport during the entire hydrograph phase as well as each step of the hydrograph. Fig. 7(a) shows that the total sediment output during the entire hydrograph does not show much difference for each experiment, indicating that the duration of conditioning flow does not pose much influence on the total volume of sediment transport during the subsequent flood.

https://doi.org/10.5194/esurf-2020-67
Preprint. Discussion started: 8 September 2020

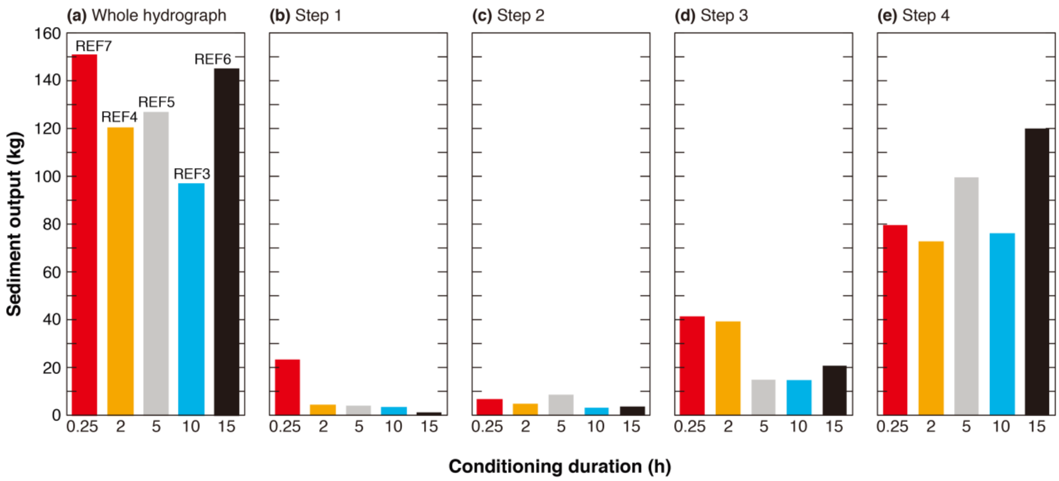

Figure 7. Sediment output measured at a trap during (a) the whole hydrograph; (b) Step 1 of the hydrograph; (c) Step 2 of the hydrograph; (d) Step 3 of the hydrograph; (e) Step 4 of the hydrograph.

However, if we study the sediment transport during each step of the hydrograph, we can find that in Step 1 REF7 (0.25) has much larger sediment output than the other experiments, as shown in Fig. 7(b). This agrees with the results for instantaneous sediment transport rate shown in Fig. 6(b), and shows that the duration of conditioning flow can influence the sediment transport at the beginning of the subsequent flood, with a longer conditioning phase lead to less sediment transport. When the duration of conditioning flow is over 2 hours, the subsequent sediment transport rate becomes rather insensitive to further increase of conditioning duration, indicating that the reorganization of the river bed under conditioning flow is mostly finished within 2 hours. The effects of stress history on subsequent sediment transport can hardly be observed during Step 2 of the hydrograph (Fig. 7(c)). Sediment output in REF7 (0.25) reduces significantly to similar magnitude of other experiments, because most of the loose bed material in REF7 (0.25) has been moved by the end of Step 1. In Step 3 of the hydrograph (Fig. 7(d)), sediment output in REF7 (0.25) and REF4 (2) is larger than in other 3 experiments which have longer conditioning phases. But this difference of sediment output among experiments is not as significant as in Step 1. In the last step of the hydrograph, with the flow discharge and sediment supply approaching their peaks, the five experiments present similar sediment outputs, demonstrating that little influence of stress history remains.

Figure 8 shows the temporal variation of the grain size distribution of the bedload. Here D_{l10}, D_{l50}, and D_{l90} denote grain sizes such that 10%, 50%, and 90% are finer in the bedload, respectively. The value of D_{l10} shows a decreasing trend during the conditioning phase (Fig. 8 (a)), with a value of more than 2 mm at the beginning to about 0.6 mm after 15 hours, in spite of the large fluctuations before 8 hours. The decrease of D_{l10} reflects an increase in the fraction of the finest sediment in bedload. In the first two steps of the hydrograph (Fig. 8(b)), the value of D_{l10} is relatively stable for experiments with long conditioning phases (i.e., REF6 (15) and REF3 (10)), but shows a decreasing trend along with fluctuations for experiments with short conditioning phases (i.e., REF7 (0.25), REF4 (2),

https://doi.org/10.5194/esurf-2020-67
Preprint. Discussion started: 8 September 2020

and REF5 (5)). The last two steps of the hydrograph see an evident increase in the value of D_{l10} compared with the first two steps, due to the increase of flow discharge and sediment supply (Fig. 8(b)).

Figures 8(c) and 8(d) show the temporal variation of D_{l50}. Compared with that of D_{l10}, the temporal variation of D_{l50} shows more significant fluctuations during the conditioning phase, as well as at the beginning of the hydrograph, and a decreasing or increasing trend for grain size in the conditioning/hydrograph phase is not as evident. As for the temporal variation of D_{l90} (in Figs. 8(e) and 8(f)), the fluctuations are still significant and there is almost no trend for either increasing or decreasing grain size during the experiment. This indicates that the transport of the coarsest sediment is not sensitive to the variation of our experimental conditions. The more significant fluctuations in D_{l50} and D_{l90} might be attributed to the fact that during relatively low flow coarse sediment is more likely to be near the threshold of motion and move intermittently, e.g. in pulses, as opposed to fine sediment. These fluctuations gradually diminish with the increase of flow and sediment supply as the static armor on bed surface transits to mobile armor.

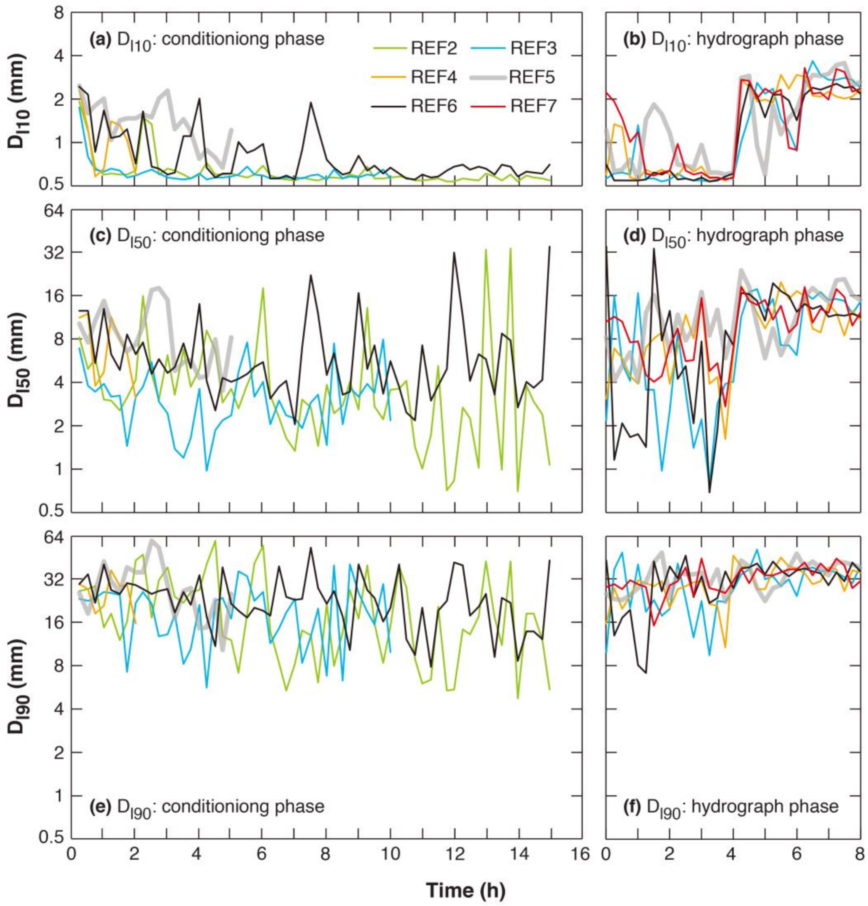

Figure 8. Temporal adjustments of characteristic grain sizes of bedload. (a) D_{l10} during conditioning phase; (b) D_{l10} during hydrograph phase; (c) D_{l50} during conditioning phase; (d) D_{l50} during hydrograph phase; (e) D_{l90} during conditioning phase; (f) D_{l90} during hydrograph phase.

https://doi.org/10.5194/esurf-2020-67
Preprint. Discussion started: 8 September 2020

With the fractional sediment transport rate measured by the light table, we also analyze the sediment mobility of each size range during the experiment. Results show that sediment transport rate is characterized by equal mobility at the beginning of the conditioning phase, but moves to partial/selective mobility after a relatively long conditioning phase as well as during the first two steps of the hydrograph. However, with the increase of flow discharge and sediment supply, the sediment transport regime gradually returns to equal mobility during the last two steps of the hydrograph. Details of the analysis are presented in the Supporting Information.

4 Discussion

4.1 Threshold of sediment motion in experiments

The threshold of sediment motion is a key parameter for the prediction of bedload transport. Previous studies on the stress history effect often start with a conditioning flow that is below the threshold of motion, and then gradually increase the flow discharge, so that the threshold of motion can be directly estimated in the experiment (e.g., Monteith and Pender, 2005; Masteller and Finnegan, 2017; Ockelford et al., 2019; etc.). Because our experiments implement a conditioning flow which can mobilize sediment (sediment transport at the beginning of the conditioning phase is especially large), the threshold of motion cannot be observed directly in the experiment. Here we estimate the threshold of sediment motion by adopting the Wong and Parker (2006) sediment transport relation, which is a revision of the Meyer-Peter and Müller (1948) relation.

We use the Wong and Parker (2006) relation, which maintains the exponent 1.5, of Meyer-Peter and Muller (1948):

$$q_s^* = 3.97\left(\tau_{s50}^* - \tau_c^*\right)^{1.5} \tag{1}$$

$$q_s^* = \frac{q_s}{\sqrt{RgD_{s50}}\,D_{s50}} \tag{2}$$

$$\tau_{s50}^* = \frac{\tau_b}{\rho g R D_{s50}} \tag{3}$$

$$\tau_b = \rho g h S_w \tag{4}$$

where q_s^* is the dimensionless bedload transport rate (Einstein number) defined by Eq. (2), τ_{s50}^* is the Shields number for surface median grain size D_{s50} defined by Eq. (3), τ_b is the flow shear stress calculated using the depth-slope product (Eq. (4)), τ_c^* is the critical Shields number for the threshold of sediment motion, q_s is the volumetric sediment transport rate per unit width; h is water depth, S_w is water surface slope, R = 1.65 is the submerged specific gravity of sediment, g = 9.81 m/s^2 is the gravitational acceleration and ρ = 1000 kg/m^3 is the water density. Wong and Parker (2006) proposed a value of 0.0495 for τ_c^* in Eq. (1). Here we obtain q_s^* and τ_{s50}^* from the measured data of the experiments, and back calculate the value of τ_c^* using Eq. (1).

https://doi.org/10.5194/esurf-2020-67
Preprint. Discussion started: 8 September 2020

Figure 9(a) shows the values of q_s^* vs. τ_{s50}^* for each experiment, along with the Wong and Parker (2006) type relation (Eq. (1)) with various values for τ_c^* (from 0.04 to 0.09). It can be seen from the figure that the measured sediment transport is relatively low, with most points below the dimensionless value of 0.001. This indicates that the Shields number in our experiment is slightly larger than the critical Shields number, a state that is typical for gravel-bed rivers (Parker, 1978). The four points with dimensionless transport rate above 0.001 are all at the beginning of the conditioning flow (t = 15 minutes). The values of q_s^* basically show an increasing trend with the increase of τ_{s50}^*, but with the value of critical Shields number τ_c^* covers a rather wide range (from less than 0.06 to larger than 0.09).

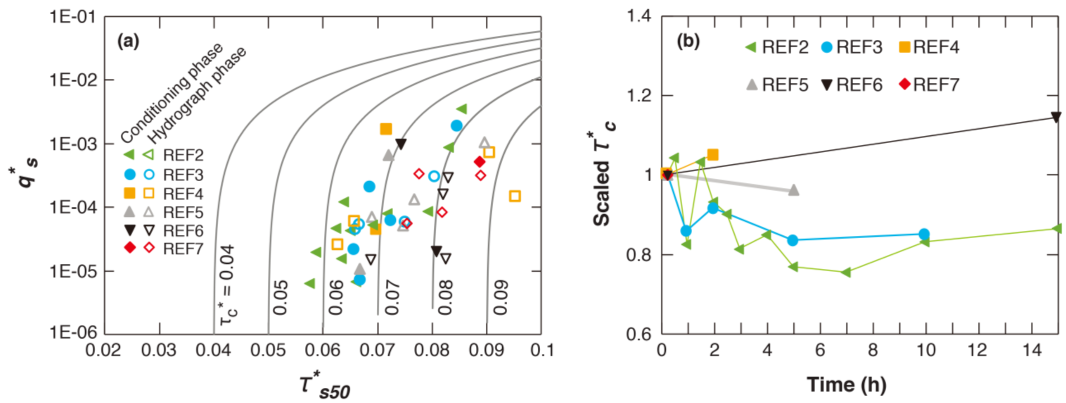

Figure 9. (a) Dimensionless sediment transport rate q_s^* vs. Shields number τ_{s50}^* using surface median grain size for measured transport rates (points). Also shown are lines for the Wong and Parker (2006) type equation (Eq. 1) using different values for τ_c^*. (b) Temporal adjustment of scaled τ_c^* (τ_c^* over τ_c^* at 15 minutes) during the conditioning phase. Here τ_c^* is back calculated using Eq. (1) (Wong and Parker (2006) type relation).

Table 2 shows the values of τ_c^* back-calculated at the beginning (t = 15 minutes) and the end of the conditioning phase in each experiment. The back-calculated values of τ_c^* vary in the range 0.066~0.086 for the conditioning phase, which is well above the value of 0.0495 as recommended by Wong and Parker (2006). Lamb et al. (2008) demonstrated that critical shear stress can become larger for large bed slope, and they proposed a relation which considers the effect of bed slope,

$$\tau_c^* = 0.15 S_b^{0.25} \tag{5}$$

where S_b is bed slope. For comparison, Table 2 also shows the values of τ_c^* calculated by Eq. (5). Results shows that for the conditioning phase of our experiments, τ_c^* calculated by Eq. (5) is above 0.06, which is much higher than the recommended value of Wong and Parker (2006) and is closer to the values back-calculated by Eq. (1). Besides, the τ_c^* values predicted by the Lamb et al. (2008) relation show little variability, indicating that only the slope effect cannot explain the observed range of τ_c^*.

https://doi.org/10.5194/esurf-2020-67
Preprint. Discussion started: 8 September 2020

Table 2. Values of τ_c^* at the beginning (t = 15 minutes) and the end of conditioning phase in each experiment. Here τ_c^* is back calculated with Eq. (1). Also shown here are values of τ_c^* estimated with the equation of Lamb et al. (2008) for comparison.

		REF2 (15)	REF6 (15)	REF3 (10)	REF5 (5)	REF4 (2)	REF7 (0.25)
t = 15 minutes	Back calculated by Eq. (1)	0.076	0.070	0.078	0.069	0.066	0.086
	Lamb et al. (2008)	0.063	0.066	0.061	0.065	0.061	0.066
End of conditioning	Back calculated by Eq. (1)	0.066	0.081	0.067	0.066	0.069	0.086
	Lamb et al. (2008)	0.061	0.063	0.060	0.063	0.062	0.066

In Fig. 9(b), we plot the scaled τ_c^* during the conditioning phase of our experiments. For each experiment, the scaled τ_c^* is calculated as the ratio between τ_c^* and the corresponding τ_c^* at t = 15 minutes. τ_c^* implemented here is back-calculated with Eq. (1). The scaled τ_c^* collapses on a value of unity at t = 15 minutes (i.e., the first point of each experiment). It can be seen from the figure that different trends are exhibited for the adjustment of τ_c^* from t = 15 minutes to the end of conditioning phase, with REF2 (15) and REF3 (10) exhibiting a decreasing trend, REF4 (2) and REF5 (5) exhibiting very slight changes, and REF6 (15) exhibiting an increasing trend. The decrease of τ_c^* in REF2 (15) an REF3 (10) is accompanied by a reduction of Shields number τ_{s50}^*, mainly due to the increase of surface median grain size D_{s50}. Moreover, the variation of back-calculated τ_c^* is mostly within a range of ±20%, in agreement with our observation that variation of bed topography and bed surface texture become insignificant after 15 minutes. It should be noted that τ_c^* cannot be back-calculated using Eq. (1) within the first 15 minutes of the conditioning phase, since the information for flow depth, water surface slope and bed surface GSD is not available. Nevertheless, we expect the adjustment of τ_c^* could be evident within the first 15 minutes, since the adjustments of both bed topography and bed surface are significant during this period (as shown in Sect. 3.1).

4.2 Implications and limitations

Previous research has shown that antecedent conditioning flow can lead to an increased critical shear stress and reduced sediment transport rate during subsequent flood event (Hassan and Church, 2000; Haynes and Pender, 2007; Ockelford and Haynes, 2013; Masteller and Finnegan, 2017; etc.). Our flume experiments also show a reduced sediment transport rate in response to the implementation of conditioning flow. However, our results are different from previous research in that the influence of antecedent conditioning flow is found to last for a relatively short time at the beginning of the following hydrograph, and then gradually diminish with the increase of flow intensity as well as sediment supply. Such results indicate that increasing flow intensity and sediment supply during a flood event can lead to the loss of memory of stress history. A similar phenomenon was observed by Mao (2018) in his experiment, where sediment transport during a high-magnitude flood event was not much affected by the occurrence of lower-magnitude flood event before.

https://doi.org/10.5194/esurf-2020-67
Preprint. Discussion started: 8 September 2020

Our results have practical implications for mountain gravel bed rivers. The importance of conditioning flow has long been discussed in the literature, and researchers have suggested that the stress history effect be considered in the modeling and analysis of gravel bed rivers. For example, previous research states that existing sediment transport theory for gravel bed rivers (e.g., Meyer-Peter and Müller, 1948; Wilcock and Crowe, 2003; Wong and Parker, 2006; etc.) might lead to unrealistic prediction if the stress history effect is not taken into account (Masteller and Finnegan, 2017; Mao, 2018; Ockelford et al., 2019). Our results indicate that the stress history effect is important and needs to be considered for low flow as well as the beginning of the flood event, but becomes insignificant as the flow gradually approaches high flow discharge. This could have implications in river engineering such as water and sediment regulation schemes for mountain gravel-bed rivers.

To explain the effect of stress history, Ockelford and Haynes (2013) has summarized the following possible mechanisms. (1) Vertical settling during the conditioning flow consolidates the bed into a tighter packing arrangement which is more resistant to entrainment. (2) Local reorientation and rearrangement of surface particles provide a greater degree of imbrication, less resistance to fluid flow, as well as direct sheltering on the bed surface. (3) The infiltration of fines into low-relief pore spaces can further increase the bed compaction. In the experiment of Masteller and Finnegan (2017), it was found that the most drastic changes during conditioning flow are manifest in the extreme tail of the elevation distribution (i.e., the highest protruding grains) and go therefore undetected in most bulk measurements (e.g. the mean bed elevation or standard deviation of bed topography). They demonstrated that such reorganization of the highest protruding grains can indeed lead to noticeable differences in the threshold of sediment transport (Masteller and Finnegan, 2017). This might explain the observation in our experiment that after the first 15 minutes of the conditioning phase, adjustments of the bed topography and the bed surface GSD become insignificant, but the sediment transport rate as well as its GSD keeps adjusting consistently.

In our experiments as well as previous experiments that study the effect conditioning flow (e.g., Monteith and Pender, 2005; Masteller and Finnegan, 2017; Ockelford et al., 2019; etc.), no sediment supply is implemented during the conditioning flow, and the flow can reorganize the bed surface to a state that is more resistant to sediment entrainment. Therefore, it is straightforward to expect that the conclusions based on our flume experiments to apply for natural rivers where sediment supply is relatively low during low flow conditions. However, some gravel-bed rivers have quite active hillslopes, and sediment input from hillslopes to river channel can occur regularly (Turowski et al., 2011; Reid et al., 2019). Since the sediment material from hillslopes is typically loose and easy to transport, under such circumstances a long inter-event duration (i.e., low-flow duration) might lead to an enhanced sediment transport rate in the subsequent flood (Turowski et al., 2011).

It should also be noted that in previous experiment on the stress history effect, conditioning flow is often set below the threshold of sediment motion. One exception is the experiment of Haynes and Pender (2007) in which the conditioning flow is above the threshold of motion for D_{50}. In this paper we also implement a conditioning flow which can mobilize sediment, especially at the beginning of the conditioning phase during which evident sediment transport occurs. Compared with the below-threshold conditioning flow, we consider that the above-threshold conditioning flow can induce more evident reorganization of bed surface, which might be more lasting during subsequent flood. That said, we expect the conclusion of this study can still hold if below-threshold conditioning flow is implemented.

https://doi.org/10.5194/esurf-2020-67
Preprint. Discussion started: 8 September 2020

Nevertheless, flume experiments with various magnitudes of conditioning flow (both above- and below-threshold of motion) merit future study. Besides, considering that the conditions of existing experiments on stress history effect are limited, implementation of numerical simulations under a wider range of conditions also merits future study.

5 Conclusions

In this paper, the effect of antecedent conditioning flow (i.e., the effect of stress history) on the morphodynamics of gravel-bed rivers during subsequent floods is studied via flume experimentation. The experiment described here is designed based on the conditions of East Creek, Canada. The experiment consists of two phases: a conditioning phase with constant water discharge and no sediment supply, followed by a hydrograph phase with hydrograph and sedimentograph. Five runs (REF 3~7) were conducted with identical experimental conditions except different durations of conditioning phase. Another run (REF 2), which consists of only the conditioning phase, is conducted in order to test the reproducibility of experimental results during the conditioning flow. Experimental results show the following.

- Adjustments of channel morphology (including channel bed longitudinal profile, standard deviation of bed elevation, characteristic grain sizes of bed surface material) are evident during the first 15 minutes of the conditioning phase, but become insignificant during the remainder of the conditioning phase.
- The implementation of conditioning flow can indeed lead to a reduction in sediment transport during the subsequent hydrograph, which agrees with previous research.
- However, the effect of stress history on sediment transport rate is limited to a relatively short time at the beginning of the hydrograph, and gradually diminishes with the increase of flow discharge and sediment supply, indicating a loss of memory of stress history under high flow discharge. Also, the effect of stress history on the GSD of bedload is not evident.
- The threshold of sediment motion is estimated with the form of the Wong and Parker (2006) relation. The estimated critical Shields number varies in the range 0.066~0.086 during the conditioning phase (excluding the first 15 minutes), and is higher than the value recommended by Wong and Parker (2006).

Our study has implications in regard to a wide range of issues for mountain gravel-bed rivers, including sediment budget analysis, river morphodynamic modeling, water and sediment regulation, flood management, and ecological restoration schemes.

Notation

D_{l50}: grain size such that 50 percent in sediment load is finer (similarly D_{l10} is such that 10 percent in sediment load is finer and D_{l90} is such that 90 percent in sediment load is finer).

D_{s50}: grain size such that 50 percent on bed surface is finer (similarly D_{s10} is such that 10 percent on bed surface is finer and D_{s90} is such that 90 percent on bed surface is finer).

F_r: Froude number.

g: gravitational acceleration.

https://doi.org/10.5194/esurf-2020-67
Preprint. Discussion started: 8 September 2020

h: water depth.

Q_s: sediment transport rate.

q_s: volumetric sediment transport rate per unit width.

q_s^*: the dimensionless bedload transport rate (Einstein number).

R: submerged specific gravity of sediment.

S_b: bed slope.

S_w: water surface slope.

ρ: water density.

τ_b: bed shear stress.

τ_c^*: critical Shields number for the threshold of sediment motion.

τ_{s50}^*: dimensionless shear stress (Shields number) of the D_{s50}.

Data availability

Data used for the analysis can be found at doi: 10.6084/m9.figshare.12758414 (An, 2020).

Author contribution

Marwan A. Hassan and Xudong Fu designed the research. Carles Ferrer-Boix performed the experiments. Chenge An processed and analyzed the experimental data. Chenge An prepared the manuscript with contributions from all coauthors.

Competing interests

The authors declare that they have no conflict of interest.

Acknowledgments

Gary Parker provided constructive comments and helped edit of this paper. Maria A. Elgueta-Astaburuaga helped conduct the experiments. Rick Ketler provided support in equipment and data collections. Eric Leinberger provided support in designing the figures. The participation of Chenge An was supported by grant from China Postdoctoral Science Foundation (grant 2018M641368). The participation of Xudong Fu was supported by grants from the National Natural Science Foundation of China (grants 51525901 and 91747207).

References

An, C.: Experimental data on sediment transport and channel adjustment in a gravel-bed river: stress history effect, doi: 10.6084/m9.figshare.12758414, 2020.

https://doi.org/10.5194/esurf-2020-67
Preprint. Discussion started: 8 September 2020

Chartrand, S. M., Jellinek, A. M., Hassan, M. A., and Ferrer-Boix, C.: Morphodynamics of a width-variable gravel bed stream: New insights on pool-riffle formation from physical experiments, Journal of Geophysical Research-Earth Surface, 123(11), 2735-2766, https://doi.org/10.1029/2017JF004533, 2018.

Chin, A., Anderson, S., Collison, A., Ellis-Sugai, B. J., Haltiner, J. P., Hogervorst. J. B., Kondolf, G. M., O'Hirok, L. S., Purcell, A. H., Riley, A. L., and Wohl E.: Linking theory and practice for restoration of steppool streams, Environmental Management, 43, 645–661, doi:10.1007/s00267-008-9171-x, 2009.

Elgueta-Astaburuaga, M. A., and Hassan, M. A.: Experiment on temporal variation of bed load transport in response to changes in sediment supply in streams, Water Resources Research, 53, 763–778, doi:10.1002/2016WR019460, 2017.

Ferrer-Boix, C. and Hassan, M. A.: Influence of the sediment supply texture on morphological adjustments in gravel-bed rivers, Water Resources Research, 50(11), 8868-8890, doi:10.1002/2013WR015117, 2014.

Ferrer-Boix, C., and Hassan, M. A.: Channel adjustments to a succession of water pulses in gravel bed rivers, Water Resources Research, 51, 8773–8790, doi:10.1002/2015WR017664, 2015.

Gomez, B. and Church, M.: An assessment of bed load sediment transport formulae for gravel rivers, Water Resources Research, 25, 1161–1186, doi:10.1029/WR025i006p01161, 1989.

Hassan, M. A., and Church, M.: Experiments on surface structure and partial sediment transport on a gravel bed, Water Resources Research, 36, 1885-1895, 2000.

Haynes, H., and Pender, G.: Stress history effects on graded bed stability, Journal of Hydraulic Engineering, 33, 343–349, 2007.

Howard, A.: A detachment-limited model of drainage basin evolution, Water Resources Research, 30(7), 2261-2285, 1994.

Johnson, J. P. L.: Gravel threshold of motion: A state function of sediment transport disequilibrium? Earth Surface Dynamics, 4(3), 685–703, https://doi.org/10.5194/esurf‐4‐685‐2016, 2016

Klingeman, P. C., and Emmett, W. W.: Gravel bedload transport processes, in: Gravel-Bed Rivers, edited by: Hey, R. D., Bathurst, J. C., and Thorne, C., John Wiley & Sons, Chichester, UK, 141-180, 1982.

Lamb, M. P., Dietrich, W. E., and Venditti, J. G.: Is the critical Shields stress for incipient sediment motion dependent on channel-bed slope? Journal of Geophysical Research-Earth Surface, 113, F02008, doi:10.1029/2007JF000831, 2008.

Mao, L.: The effects of flood history on sediment transport in gravel bed rivers, Geomorphology, 322, 192–205, https://doi.org/10.1016/j.geomorph.2018.08.046, 2018.

Marston, R. A.: Land, life, and environmental change in mountains, Annals of the Association of American Geographers, 98, 507–520, https://doi.org/10.1080/00045600802118491, 2008.

Masteller, C. C., and Finnegan, N. J.: Interplay between grain protrusion and sediment entrainment in an experimental flume, Journal of Geophysical Research-Earth Surface, 122, 274–289, https://doi.org/10.1002/2017GL076747, 2017.

Earth Surface Dynamics Discussions

Masteller, C. C., Finnegan, N. J., Turowski, J. M., Yager, E. M., and Rickermann, D.: History dependent threshold for motion revealed by continuous bedload transport measurements in a steep mountain stream, Geophysical Research Letters, 46, 2583–2591, 2019.

Monteith, H., and Pender, G.: Flume investigation into the influence of shear stress history, Water Resources Research, 41, W12401, https://doi.org/10.1029/2005WR004297, 2005.

Montgomery, D. R., and Buffington, J. M.: Channel ‑ reach morphology in mountain drainage basins, Geological Society of America Bulletin, 109(5), 596–611, https://doi.org/10.1130/0016 ‑ 7606(1997)109<0596:CRMIMD>2.3.CO;2, 1997.

Montgomery, D. R., Buffington, J. M., Peterson, N. P., Schuett-Hames, D., and Quinn, T. P.: Stream-bed scour, egg burial depths, and the influence of salmonid spawning on bed surface mobility and embryo survival, Canadian Journal of Fisheries and Aquatic Sciences, 53, 1061–1070, 1996.

Meyer-Peter, E., and M üller, R.: Formulas for bed-load transport, in: Proceedings of the 2nd Congress of International Association for Hydraulic Structures Research, Stockholm, Sweden, 7-9 June 1948, 39-64, 1948.

Ockelford, A., and Haynes, H.: The impact of stress history on bed structure, Earth Surface Processes and Landforms, 38, 717–727, https://doi.org/10.1002/esp.3348, 2013.

Ockelford, A., Woodcock, S., and Haynes, H.: The impart of inter-flood duration on non-cohesive sediment bed stability, Earth Surface Processes and Landforms, 44, 2861-2871, doi:10.1002/esp.4713, 2019.

Paola, C., Heller, P. L., and Angevine, C. L.: The large-scale dynamics of grain-size variation in alluvial basins, I: Theory, Basin Research, 4, 73–90, 1992.

Papangelakis, E., and Hassan, M. A.: The role of channel morphology on the mobility and dispersion of bed sediment in a small gravel-bed stream, Earth Surface Processes and Landforms, 41, 2191–2206, 2016.

Paphitis, D., and Collins, M. B.: Sand grain threshold, in relation to bed stress history: an experimental study, Sedimentology, 52, 827–838, 2005.

Parker, G.: Self-formed straight rivers with equilibrium banks and mobile bed. Part 2. The gravel river, Journal of Fluid Mechanics, 89, 127-146, 1978.

Parker, G.: 1D sediment transport morphodynamics with applications to rivers and turbidity currents, available at: http://hydrolab.illinois.edu/people/parkerg//morphodynamics_e-book.htm, 2004.

Powell, D. M., Reid, I., and Laronne, J. B.: Hydraulic interpretation of crossstream variations in bed-load transport, Journal of Hydraulic Engineering, 125, 1243–1252, 1999.

Reid, D. A., Hassan, M. A., Bird, S., and Hogan D.: Spatial and temporal patterns of sediment storage over 45 years in Carnation Creek, BC, a previously glaciated mountain catchment, Earth Surface Processes and Landforms, 44, 1584-1601, doi: 10.1002/esp.4595, 2019.

Reid, I., and Frostick, L. E.: Particle interaction and its effects on the thresholds of initial and final bedload motion in coarse alluvial channels, in: Sedimentology of Gravels and Conglomerates-Memoir 10, edited by: Koster, E. H., and Steel, R. J., Canadian Society of Petroleum Geologists, Calgary, Canada, 61–68, 1984.

Reid, I., Frostick, L. E., and Layman, J. T.: The incidence and nature of bedload transport during flood flows in coarse-grained alluvial channels, Earth Surface Processes and Landforms, 10, 33–44, 1985.

Rickenmann, D.: Comparison of bed load transport in torrents and gravel bed streams, Water Resources Research, 37, 3295–3305, doi:10.1029/2001WR000319, 2001.

Schneider, J. M., Rickenmann, D., Turowski, J. M., Bunte, K., and Kirchner, J. W.: Applicability of bed load transport models for mixed-size sediments in steep streams considering macro-roughness, Water Resources Research, 51, 5260–5283, doi:10.1002/2014wr016417, 2015.

Sklar, L., and Dietrich W. E.: A mechanistic model for river incision into bedrock by saltating bed load, Water Resources Research, 40, W06301, doi:10.1029/2003WR002496, 2004.

Turowski, J. M., Badoux, A., and Rickenmann, D.: Start and end of bedload transport in gravel-bed streams, Geophysical Research Letters, 38, L04401, https://doi.org/10.1029/2010GL046558, 2011.

Whiting, P. J., and Dietrich, W. E.: Boundary shear stress and roughness over mobile alluvial beds, Journal of Hydraulic Engineering, 116, 1495–1511, 1990.

Wilcock, P. R., and Crowe, J. C.: Surface-based transport model for mixed-size sediment, Journal of Hydraulic Engineering-ASCE, 129, 120–128, doi:10.1061/(asce)0733-9429(2003)129:2(120), 2003.

Wong, M., and Parker, G.: Reanalysis and correction of bed-load relation of Meyer-Peter and Müller using their own database, Journal of Hydraulic Engineering-ASCE, 132, 1159–1168, doi:10.1061/(ASCE)0733-9429(2006)132:11(1159), 2006.

Yager, E. M., Turowski, J. M., Rickenmann, D., and McArdell, B. W.: Sediment supply, grain protrusion, and bedload transport in mountain streams, Geophysical Research Letters, 39, L10402, https://doi.org/10.1029/2012GL051654, 2012.

Zimmermann, A., Church, M., and Hassan, M. A.: Video-based gravel transport measurements with a flume mounted light table, Earth Surface Processes and Landforms, 33(14), 2285-2296, https://doi.org/10.1002/esp.1675, 2008.